IMPROVING ESA'S COLLISION RISK ESTIMATES BY AN ASSESSMENT OF THE TLE ORBIT ERRORS OF THE US SSN CATALOGUE

T. Flohrer[1], H. Krag[2], H. Klinkrad[2], B. Bastida Virgili[2], and C. Früh[3]

[1] *Aboa Space Research Oy (ASRO) at ESA/ESOC Space Debris Office, Robert-Bosch-Straße 5, DE-64293 Darmstadt, Germany, Email: tim.flohrer@esa.int*

[2] *ESA/ESOC Space Debris Office, Robert-Bosch-Straße 5, DE-64293 Darmstadt, Germany, Email: holger.krag@esa.int, heiner.klinkrad@esa.int, benjamin.bastida.virgili@esa.int*

[3] *Astronomical Institute University of Bern, Sidlerstrasse 5, CH-3012 Bern, Switzerland, Email: carolin.frueh@aiub.unibe.ch*

ABSTRACT

The Space Debris Office at ESA predicts conjunction events and assesses the associated collision risk. Upcoming high-risk conjunction events are identified based on Two-Line element (TLE) data obtained from the US Space Surveillance Network (SSN) and the precisely known orbits and covariance information of the supported missions. This analysis faces the problem that no covariance information is available for the TLE sets. We estimate the uncertainties of the TLE orbit model in radial, along-track, and out-of-plane coordinates for several complete snapshots of the TLE-catalogue by comparing states derived directly from the TLE data with states resulting from an orbit determination using pseudo-observations derived from TLE data. We validate the result for selected objects by comparing the TLE orbit uncertainties to orbit errors estimated in a similar way from precise ephemerides. The considered precise ephemerides are predicted orbits utilised by the International Laser Ranging Service for tracking satellites equipped with retro-reflectors, as well as from precisely determined orbits of some objects in GEO, regularly tracked from the Zimmerwald observatory of the Astronomical Institute of the University of Bern. We further consider precise orbits that were determined from radar tracking of chaser objects involved in high-risk conjunction events.

Key words: Collision Avoidance, Collision Risk Assessment, Two-Line Elements .

1. INTRODUCTION

ESA's Space Debris Office located at ESOC predicts conjunction events routinely for currently two ESA missions, the Low-Earth orbiting satellites ERS-2 and ENVISAT. Orbital information of potential chaser objects are received from the US Space Surveillance Network (SSN) and provided in the Two-Line element (TLE) format. The collision risk of the covered missions is assessed for all conjunction events that are identified though a filtering process applied to the TLE data. The results of this assessment of the collision risk are distributed in a daily bulletin.

ESA uses the tool CRASS (Collision Risk Assessment Software, [1] and [2]) to identify conjunction events and to estimate the associated collision risk. Dedicated tracking of the identified chaser object is acquired if the assessed collision risk qualifies the conjunction event as a "high-risk conjunction event". An improved orbit determined from these tracking data gives improved state and covariance information of the chaser object. Using this updated information, a re-assessment of the collision risk with CRASS allows to decide on the necessity of collision avoidance manoeuvres and to support the planning of necessary manoeuvres. The applied widely automated process is described in detail in [3].

The risk assessment of collisions in space in general, not only through CRASS, faces the problem that no covariance information is available for the TLE data set. The risk assessment requires the propagation of orbital states and covariance information of the identified chaser to the estimated conjunction epoch. The design of CRASS addresses this central issue by introducing pre-defined look-up tables for the initial covariance (valid at the epoch of the TLE data set) that are sorted by eccentricity, perigee height and inclination. The used look-up tables are filled with covariance information of a limited number of representative objects. That information is obtained from comparing states derived directly from the TLE data with states resulting from an orbit determination using pseudo-observations derived from TLE data. The obtained covariance information reflects the limitations of the TLE orbit model combined with limitations in the orbit determination and orbit propagation accuracy. The term "TLE uncertainties" better describes this covariance information, whereas the estimation of "TLE errors" requires information from an validation of the propagated TLE states.

Proc. '5th European Conference on Space Debris', Darmstadt, Germany 30 March – 2 April 2009, (ESA SP-672, July 2009)

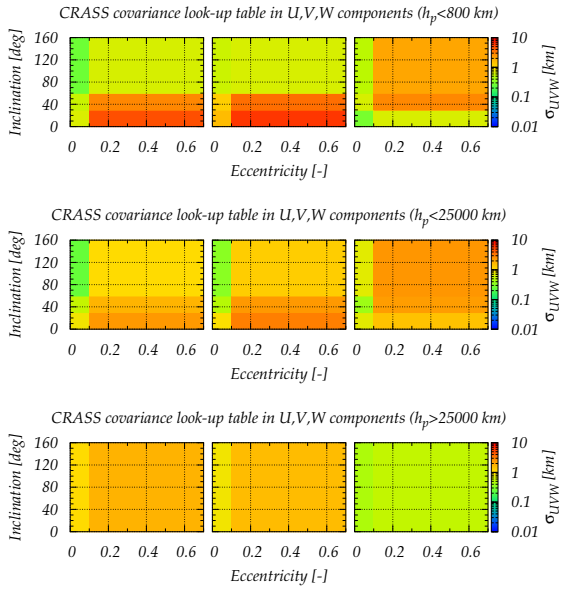

Figure 1. Covariance information stored in the look-up-table of CRASS in radial (U), along-track (V), and out-of-plane (W) components, shown as function of perigee height h_p, eccentricity e, and inclination i (σ_U: left, σ_V: centre, σ_W: right).

In this work we present an approach to extending the covariance look-up table to consider the entire SSN catalogue. We compare the internal TLE orbit uncertainties for several complete snapshots of the TLE-catalogue. This analysis is complemented by validating the obtained TLE orbit uncertainties for selected objects. This work is motivated by the fact that any improvement of the data stored in the look-up-tables used by CRASS would results in a better decision baseline whether or not to perform collision avoidance manoeuvres. It would also contribute to meeting the goal of keeping the use of external tracking facilities at a minimum.

This work not only reports on the ongoing improvements in ESA's conjunction event detection and collision risk assessment process. It also provides insights into the applicability of the TLE theory to certain classes of orbits. The latter is in particular interesting for the discussion of data products and formats for the future European Space Situational Awareness System that is under study.

2. TLE ORBIT UNCERTAINTIES

2.1. Applied Methodology

This section describes the used method for deriving the TLE orbit uncertainties to improve the covariance look-up tables. We extend the "numerical fit" method that was used to generate the covariance look-up tables of CRASS. This method uses the tool ODIN (see [4]) to compare states derived directly from the TLE data via the SGP theory to states resulting from an orbit determination using pseudo-observations. Those pseudo-observations are derived from a numerical propagation of the state at the TLE epoch through ODIN. The desired covariance information is obtained from the statistical analysis of the residuals from the comparison in the UVW-space (radial, along-track, out-of-plane) over a certain time span (24 hours). The original method was based on manually processing a limited number of 14 objects, each one found representative for one class in the space inclination - eccentricity - perigee height. Figure 1 gives a graphical representation of the resulting look-up table used in CRASS. Later this approach was applied to 21 objects with a perigee height below 450 km [5], confirming the previous results. The applied methodology is outlined in detail in [4].

We now apply this procedure to the entire TLE catalogue, which became feasible after a recent upgrade of the processing environment [3]. We compare ephemerides spanning 24 hours each, centred at the TLE-epoch. The orbit determination and the numerical propagation of the determined states over the 24 hours arc consider the MSIS-90 atmospheric model, luni-solar perturbations, solar radiation pressure, and the Earth's gravity field modeled up to degree and order 30 (JGM3). Area and mass of the satellite are taken from ESA's DISCOS database. If those values are not available default values of 10 kg and 1 m^2 are used. Finally, we calculate the standard deviation of the residuals between the two orbits in the UVW-space (σ_U, σ_V, and σ_W) as input for the generation of the covariance look-up tables. Hence, the obtained covariance information reflects the limitations of the TLE orbit model. In principle, ODIN's limitations in terms of orbit determination, orbit propagation accuracy, and generation of pseudo observations are also included in this result, but might be neglected as outlined in [6]. Ref. [6] also outlines in detail the set-up of our experiment.

2.2. Other Methods

Alternative approaches to estimate covariance information for TLEs exist. The optimal approach would be to compare TLE-based ephemerides to operational orbits obtained from satellite operators. This is impossible for the vast majority of objects in orbit. For some objects at least the comparison to high-accuracy (post-processed) orbits may be possible, as for some satellites such orbits are available from coordinated efforts of the scientific community (such as the IGS, ILRS, IDS, etc.). But still only a very limited number of satellites may be covered, showing large gaps in some orbital regions. We will apply this method to some available objects in the next section to validate the obtained TLE uncertainties.

A method that could be applied to the entire catalogue of objects is to compare ephemerides generated by subse-

quent TLE-sets, allowing to estimate the covariance information from the differences in the overlapping arcs, in particular at both TLE epochs. This method is applied in the routine conjunction analyses and collision risk estimates at CNES [7]. This method only gives the TLE accuracy if the TLEs are unbiased. Some limitations of the TLE theory may not be detected with this approach, as successive TLE-sets would still be correlated. This method directly reveals, however, inconsistencies between the analysed TLEs, as due to orbital manoeuvres, which is not possible with our selected method.

Previous studies at ESOC recommended to use the "numerical fit" approach for the conjunction event detection and collision risk assessment service covering the ESA satellites [5], as the results were found closer to the mean value of states obtained from operational orbits. The additional consideration of the "overlap" approach might, however, help to increase confidence.

Finally, covariance information may be obtained from trying to reconstruct raw observations of the particular object, that might be used to generate the TLE. This attempt requires (at least) reasonable assumptions on the TLE production process, in particular on the acquiring sensor and the data acquisition epochs, the measurement errors and potentially biases of those sensor. This step should be considered as an additional step to the other presented methods.

2.3. Results for various snapshots

All TLE data used in our analyses was taken from ESA's DISCOS database [8] that contains orbital elements in TLE format together with additional information for Earth-orbiting objects. The source of the TLE sets is the US Space Surveillance Network. A total of eight snapshots of the TLE catalogue were generated using the TLE-set nearest to the reference epoch, with cut-offs at 30 days prior and after that epoch. The considered reference epochs were 1990 Jul 01, 1993 Jan 01, 1995 Jul 01, 1998 Jan 01, 2000 Jul 01, 2003 Jan 01, 2005 Jul 01, and 2008 Jan 01. The 2008 Jan 01 snapshot of the TLE catalogue consists of 11470 individual objects, of which 11286 were successfully processed with our method.

The resulting covariance information estimated for this most recent snapshot is given in Fig. 2. Standard deviations of the residuals of up to about 5 km are possible in certain regions in the along-track direction. Both, the radial and out-of-plane components show smaller uncertainties compared to the along-track component. This result is expected, as in the along-track component the insufficiencies of the drag modelling show up most prominently (for LEOs), as well as epoch registration errors contained in the observations. In general, objects in low-eccentric orbits seem to be covered better by the TLE-theory than objects in orbits with higher eccentricities. We may also identify a dependency on the inclination. Leaving the near-circular orbits out, objects in low-inclined orbits show higher uncertainties in radial and along-track direction compared to objects orbiting in higher inclinations. The reason for a different pattern in the out-of-plane component is unknown. The largest uncertainties in out-of-plane are found at medium inclination values, centred at $i \approx 40^\circ$. Further investigations might consider the bridging of gaps in the observability of these objects, and might include assumptions on the performance of the used sensors.

Table 1. Tabulated results of the analysis of the TLE catalogue of the epoch 2008 Jan 01 in radial (U), along-track (V), and out-of-plane (W) components (the ratio used vs. total number of objects refers to a 6-sigma filtering for outliers).

Orbit regime	Objects (used/total)	Averaged $\sigma_U[km]$	Averaged $\sigma_V[km]$	Averaged $\sigma_W[km]$
LEO	8454/8463	0.102	0.471	0.126
MEO	317/321	0.073	0.131	0.054
GTO	371/371	1.960	3.897	1.808
HEO	1237/1245	0.824	1.367	1.059
GEO	878/886	0.359	0.432	0.086

In order to compare the results from the analyses of different snapshots we classify the objects according to their orbits (h_A - apogee altitude, h_P - perigee altitude) :

- LEO (Low-Earth orbits):
  $h_A < 2000$ km
- GEO (Geostationary orbits):
  $h_P > 33786$ km and $h_A < 37786$ km
- MEO (Medium-Earth orbits):
  $h_P > 2000$ km and $h_A < 33786$ km
- GTO (Geostationary transfer orbits):
  $h_P < 2000$ km and $h_A > 33786$ km
- HEO (Highly elliptical orbits):
  all other objects

According to this classification scheme we may average the estimated values for the standard deviation in the UVW-space. For the 2008 Jan 01 snapshot the averaged values for the three analysed components are given in Tab. 1. All results for a certain class of objects were filtered for outliers using a 6-sigma criterion. Further, the number of total and used (i.e. non-rejected) objects is given.

In LEO and MEO the lowest TLE uncertainties might be expected. In particular for the orbits of navigation satellites (circular orbits with inclination around 50°-60°) in MEO the TLE uncertainties are extremely low in all components. A close-up of the LEO region (compare with Fig. 3) reveals that the radial and the out-of-plane component are described similarly well for near-circular orbits, while uncertainties reach up to 0.4 km for the remaining objects. The uncertainties in along-track component

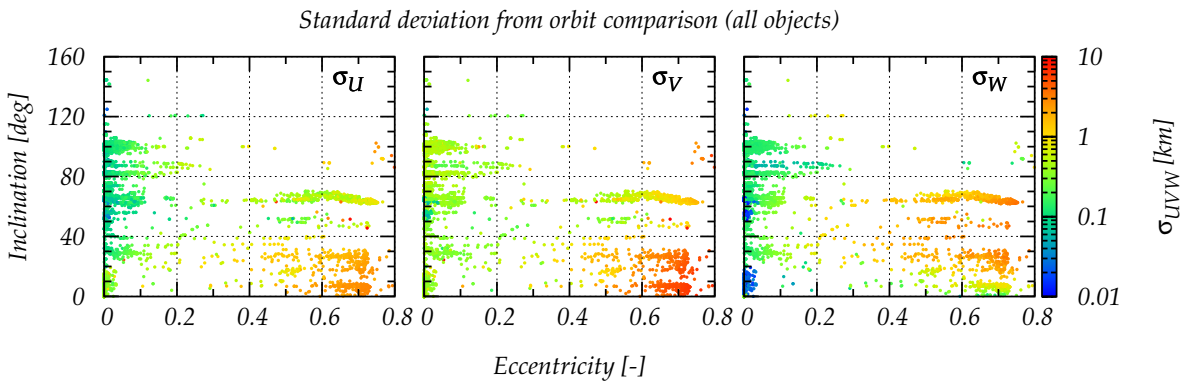

Figure 2. Covariance information estimated from the 2008 Jan 1 snapshot as function of eccentricity e, and inclination i, in radial (U), along-track (V), and out-of-plane (W) components.

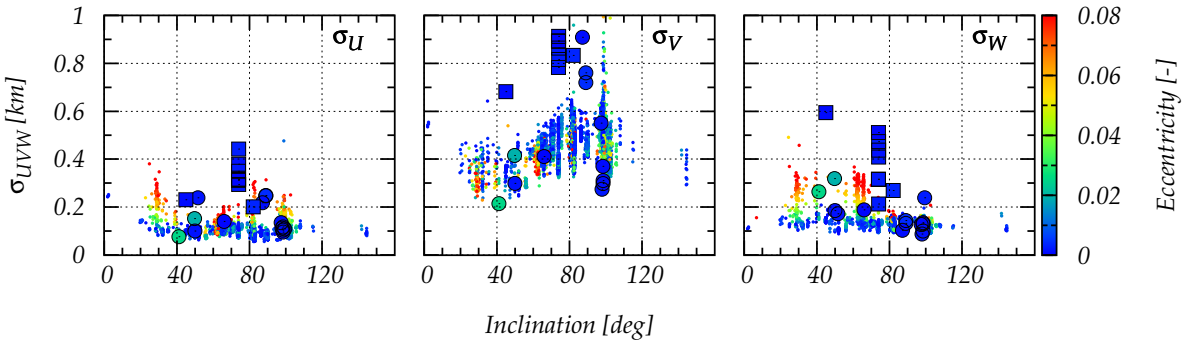

Figure 3. Inclination i vs. covariance information in radial (U), along-track (V), and out-of-plane (W) components with colour-coded eccentricity e, for LEO objects ($h_A < 2000$ km), as estimated from the 2008 Jan 1 snapshot . Results for the comparison with precise ephemeris from CPFs are given as circles, while squares correspond to comparisons with propagated states of tracked objects involved in high-risk conjunction events.

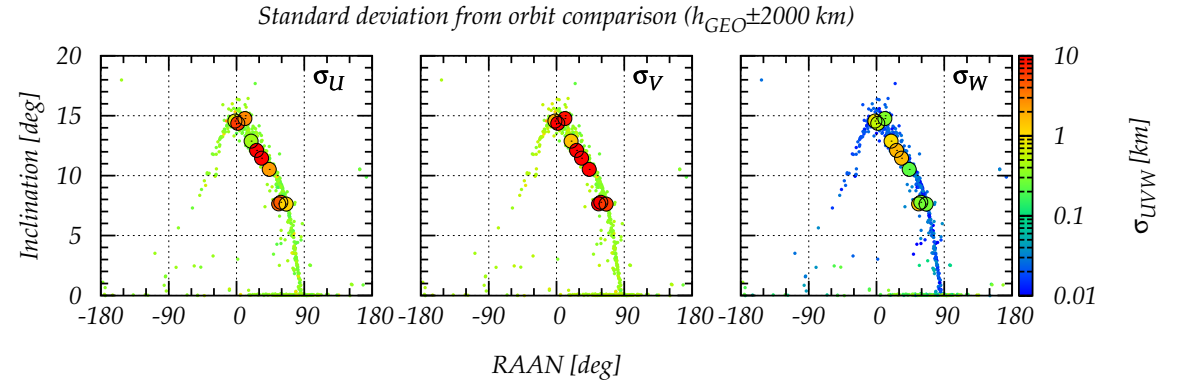

Figure 4. Covariance information estimated from the 2008 Jan 1 snapshot for GEO objects ($h_{GEO} \pm 2000$ km) as function of right ascension of ascending node $RAAN$, and inclination i, in radial (U), along-track (V), and out-of-plane (W) components. Results for the comparison with precise orbits are given as circles (indicating objects from the Zimmerwald catalogue).

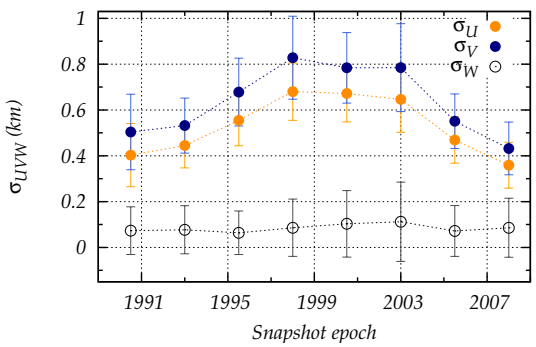

Figure 5. Comparison of several historical snapshots of the estimated uncertainties of the GEO objects in radial (U), along-track (V), and out-of-plane (W) components. The assigned error bars denote the standard deviation of the averaged value resulting from the averaging process.

show a dependency from the inclination, and reach typically up to 0.6 km for high inclination values. There seems to be no variation as function of the eccentricity in the along-track component.

Analysing the objects of the GTO and HEO class shows that eccentric, low inclination orbits have large uncertainties in the radial and along-track component, while the uncertainties in the out-of-plane component are comparably moderate. From all objects in eccentric orbits those orbiting in the inclination band between 60° and 65° have a significantly lower uncertainty in the radial and along-track component, but have a higher uncertainty in the radial component. This might indicate that these two groups are covered by different sensors, are observed with different priorities, and/or that there are other systematic effects in the TLE-generation process affecting mostly the GTOs in low inclination orbits.

The GEO class is analysed in the RAAN (right ascension of the ascending node) vs. inclination space, as for objects in the GEO class the eccentricity is always low. In the 2008 snapshot the uncertainties in the along-track and in the radial component are both below 0.5 km (see Tab. 1 and Fig. 4). The radial component that is found better than 0.1 km, with the exception of active (e.g. manoeuvring) objects with $i \approx 0°$.

The comparison of the averaged standard deviation in the UVW-space per class and component for different snapshots shows no significant changes over time for the LEO and MEO classes. This is different for the GEO region. According to Fig. 5 the along-track and radial component are worse by a factor of ≈1.5 between 1995 and 2003, but are steadily improving since 2003. The out-of-plane component is not affected. The reason for this signal is unclear.

3. VALIDATION OF THE OBTAINED TLE ORBIT UNCERTAINTIES FOR SELECTED OBJECTS

3.1. Methodology

The obtained TLE uncertainties may be validated by comparing the states, propagated directly from TLEs, to precise ephemerides. We may use the identical framework as for the estimation of the TLE uncertainties by replacing the ephemerides from the "numerically fitted" orbit by the precise ephemerides. One source of such ephemerides are those orbits determined from radar tracking data, acquired to support the analysis of high-risk conjunction events of ENVISAT and ERS-2 during the last three years [3]. We used the tracking data and the determined orbit for nine of these chaser objects. The tracking data usually consists of at least three tracks acquired during two subsequent days by the radar system TIRA (Tracking and Imaging Radar), operated by FGAN (Forschungsgesellschaft für Angewandte Naturwissenschaften). Precisely determined states with reliable covariance information are obtained from processing those radar tracks, with the range residuals w. r. t. the radar tracking determined to be below ≈20 m. We also include the precisely determined orbit of the XMM satellite into the analysis, which was obtained from combining optical and radar tracking data acquired during the XMM contingency in October 2008 [9].

Additional precise ephemeris maybe obtained from predicted orbits given in the Consolidated Prediction Format (CPF), utilised by the ILRS (International Laser Ranging Service) for tracking satellites equipped with retro-reflectors. The ILRS provides satellite ranging data for most of the satellites equipped with laser retro-reflectors [10]. Such satellites orbit in very different orbital regimes, mostly in LEO and MEO. For all tracked satellites, based on acquired tracking data, the so-called analysis centers (ACs) routinely update their predictions for upcoming laser tracking attempts. Each AC produces own prediction, but not all ACs cover all tracked satellites with predictions. All predictions follow requirements of the Consolidated Laser Ranging Prediction (CPF)-format, which basically are tabulated geocentric, earth-fixed states in the International Terrestrial Reference Frame (ITRF). CPFs were found available back to 2005 [11]. To be able to compare the CPF-data with the TLE-based ephemeris, a conversion is applied to transform the CPF-data from the earth-fixed system to the true equator mean equinox (TEME) system of the TLEs. This transformation takes into account the sidereal time and the polar motion.

Unfortunately, the ILRS does not provide the determined orbits that are used to generate the CPF predictions, and also the accuracy of the predictions is unknown. It is, however, assumed that the accuracy depends on the satellite-dependent tracking scheme, the limitations set by the observation technique, the weather situation and the availability of tracking stations in general. For this

Table 2. Comparison of precise post-processed orbits for ERS-2 and ENVISAT with CPF-based propagation results (1-σ RMS). U - radial, V - along-track, W - out-of-plane component.

Satellite	Epoch	σ_U (km)	σ_V (km)	σ_W (km)
ENVISAT	30 Nov 2007	0.001	0.022	0.005
ENVISAT	19 Dec 2007	0.002	0.033	0.007
ENVISAT	15 Sep 2008	0.000	0.009	0.007
ERS-2	14 Jul 2008	0.001	0.014	0.010

reason, the first experiment of the study was to assess the CPF accuracy for exemplary satellites. As ENVISAT and ERS-2 are two of the laser tracked satellites, highly precise post-processed orbits of these satellites have been obtained from the ESOC's Navigation Office. In fact, these orbits were used to generate ESOC's CPF-data for ENVISAT and ERS-2. The comparison between these precise orbits and the CPFs from 3 different centers and for 4 different epochs (30 Nov 2007, 20 Dec 2007, 15 Jul 2008 and 16 Sep 2008) shows that the predicted orbits are precise with a maximal error of less than 40 m in along-track direction and below 10 m for the radial and out-of-plane component, see Tab. 2. We may thus assume the CPF predictions to be sufficient to analyse the accuracy of the TLE-based ephemeris.

Finally, in order to study also higher altitudes, as the GEO region, we propagated the precisely determined orbits of some objects in GEO, which are regularly tracked from the Zimmerwald observatory of the AIUB.

For all validation attempts we selected the TLE-set from DISCOS that is nearest to the available precise orbit. The epoch difference may only for the GEO objects reach up to several ($<$7) days.

3.2. Results for LEO objects

Tab. 3 gives details for the considered objects used for the validation of the estimated TLE uncertainties. In the LEO region CPFs of the following objects were used: Ajisai, ANDE-RR Active and Passive, Beacon-C, CHAMP, ENVISAT, ERS-2, GRACE-A, GRACE-B, Gravity Probe B, Jason-1, Jason-2, Meteor-3M, LAGEOS-1, LAGEOS-2, Larets, Starlette, Stella, and TerraSAR-X. We considered six different epochs of CPFs, which are 29/12/2005, 26/06/2006, 28/12/2006, 13/07/2007, 27/12/2007, and 26/06/2008. Some of these satellites may carry out manoeuvres. Such epochs are excluded from the analysis. Tab. 3 also lists the nine objects that were tracked by TIRA during the analysis of upcoming high-risk conjunction events. These chaser objects are often COSMOS satellites, resulting in a clustering at $i \approx 74^\circ$. We highlight the validation results also in Fig. 3 by overlaying the results with similarly colour-coded circles and squares, each representing one validation result.

Tab. 3 and Fig. 3 show that in principle the validation confirms the estimated TLE uncertainties in LEO. The CPF-based uncertainties are slightly worse than the averaged values for the LEO regime for the objects in the orbits with $i \approx 89^\circ$ or $i \approx 50^\circ$. The results for the chaser objects involved in high-risk conjunction events indicate a significant difference, as the standard deviations are worse by a factor of about 2 compared to the estimated TLE uncertainties. It needs to be discussed further, whether this is due to a systematic effect in the TLE generation process for orbits with $i \approx 74^\circ$. We need to factor in that these chaser orbits are determined from a few short passes only, which is sufficient for the original purpose - to precisely determine states and to obtain accurate and reliable covariance information. Some perturbation effects might not, however, be fully addressable from the tracking geometry, which would in turn degrade the quality of the statistical analysis of the residuals from the comparison in the UVW-space over 24 hours. We already observed that the TLE uncertainties vary as function of the inclination, most prominently in the along-track component, and may at least conclude that the results are too optimistic for some inclination bands.

3.3. Results for GEO objects

In addition to the objects in LEO, Tab. 3 provides details about the 10 objects in the GEO region. Those objects, of which none is an active satellite, are regularly observed in Zimmerwald in the scope of different ongoing projects. Here we considered arc lengths of several days - usually about 2 weeks. The orbit determination was carried out by AIUB and results in orbits better than $1\farcs0$, usually better that $0\farcs5$ in equatorial coordinates, which corresponds to $\approx$100 m in the GEO region. Using ephemerides obtained from propagating these precise orbits to validate the estimated TLE uncertainties in the GEO region reveals that the estimated TLE uncertainties might be too optimistic, as Fig. 4 together with Tab. 3 indicates. Usually, the uncertainties in the radial and along-track component differ by one order of magnitude, but for 3 objects (80081A, 83089B, 85035B) they differ even more. The out-of-plane component is not always the best determined component, which was unexpected for the GEO region.

The large differences for some objects might either correspond to limits of the TLE theory, or to limits in the observation technique applied. The latter seems unlikely, as the orbit determination results indicate a good fit of the observations. Further studies are underway that address the fact that a TLE-set does not indicate whether or not the orbit was improved using new observations, or the TLE-set is the result of a propagation only. We may add that optical observations carried out at Zimmerwald observatory and with ESA's Space Debris Telescope at Tenerife, Spain, indicate that observed astrometric positions may be off up to 0.1° in longitude and latitude, compared to the TLE-based predicted positions, which would correspond to an offset of about 70 km in combined along-track/out-of-plane position. This is also supported by [12], who observed a scattering of several kilo-

Table 3. Comparison of all considered precise CPF ephemerides, ephemerides from radar tracking and optical tracking data to TLE-based ephemerides: approximate orbital elements (a - semi-major axis, e - eccentricity, i - inclination) and determined standard deviation of differences in radial (U), along-track (V), and out-of-plane (W) components. Results for CPF ephemerides are averaged over all considered CPFs (indicated by n_{CPF}). Optical tracking data is described via the length of the observed arc, the number of observations n_{obs}, and the obtained RMS from the orbit determination.

Satellite (km)	Source (-)	n_{CPF} (°)	n_{Tracks} (km)	Arc length(d) (km)	a (km)	e	i	σ_U	σ_V	σ_W
65032A	CPF	10	-	-	7492	0.025	41.2	0.077	0.215	0.265
75010A	CPF	12	-	-	7339	0.020	49.8	0.153	0.416	0.319
76039A	CPF	15	-	-	12273	0.004	109.9	0.075	0.302	0.174
86061A	CPF	14	-	-	7864	0.002	50.0	0.101	0.300	0.186
92070B	CPF	15	-	-	12159	0.014	52.6	0.178	0.443	0.437
93061B	CPF	12	-	-	7169	0.001	98.4	0.105	0.370	0.135
95021A	CPF	14	-	-	7154	0.001	98.6	0.097	0.299	0.131
00039B	CPF	18	-	-	6706	0.001	87.2	0.219	0.909	0.104
01055A	CPF	15	-	-	7715	0.001	66.0	0.141	0.412	0.189
01056A	CPF	1	-	-	7388	0.003	99.4	0.110	2.852	0.240
02009A	CPF	16	-	-	7159	0.001	98.5	0.118	0.311	0.101
02012A	CPF	10	-	-	6834	0.004	89.0	0.249	0.760	0.133
02012B	CPF	10	-	-	6833	0.004	89.0	0.248	0.720	0.145
03042G	CPF	16	-	-	7060	0.002	98.0	0.113	0.275	0.088
06055F	CPF	2	-	-	6677	0.002	51.7	0.240	1.463	0.173
07026A	CPF	4	-	-	6892	0.002	97.4	0.136	0.550	0.128
71114B	Radar	-	4	-	7143	0.002	74.0	0.295	0.864	0.409
78105A	Radar	-	6	-	7160	0.003	74.1	0.443	1.285	0.474
82051A	Radar	-	4	-	7158	0.002	74.0	0.317	0.783	0.316
83063B	Radar	-	3	-	7146	0.004	82.1	0.202	0.833	0.270
83079A	Radar	-	5	-	7157	0.002	74.0	0.380	0.912	0.438
85006A	Radar	-	4	-	7154	0.002	74.0	0.350	0.894	0.318
85006B	Radar	-	4	-	7150	0.003	74.1	0.317	0.816	0.214
94083B	Radar	-	3	-	7159	0.001	74.0	0.312	0.891	0.511
98053H	Radar	-	4	-	7175	0.001	45.0	0.231	0.682	0.595
99066A	Rad/Opt	-	1	0.2 (126, 0.″44)	66924	0.583	57.8	12.123	20.596	9.615
79105A	Optical	-	-	15 (174, 0.″49)	42177	0.001	14.6	0.772	1.603	0.891
80081A	Optical	-	-	16 (56, 0.″23)	42170	0.000	14.4	6.061	12.495	0.569
82044F	Optical	-	-	16 (72, 0.″27)	42166	0.001	14.8	2.880	5.711	0.318
83089B	Optical	-	-	19 (90, 0.″29)	42148	0.001	11.5	11.349	22.910	1.660
84035A	Optical	-	-	15 (266, 0.″81)	42185	0.001	12.9	0.394	1.037	0.964
85035B	Optical	-	-	24 (200, 0.″35)	42141	0.001	12.1	10.099	19.991	1.731
90061D	Optical	-	-	10 (92, 0.″46)	42147	0.003	10.5	2.336	5.639	0.228
91010F	Optical	-	-	10 (122, 0.″15)	42203	0.002	7.6	4.184	8.421	1.411
92088A	Optical	-	-	16 (66, 0.″30)	42138	0.000	7.8	4.508	9.646	0.329
99047E	Optical	-	-	14 (50, 0.″18)	42197	0.010	7.6	1.148	2.165	0.277

meters in the TLE-based prediction of miss distances in GEO. The authors compared positions based on TLE predictions to those obtained from optical multi-site observations.

4. SUMMARY

We have presented an approach to improve ESA's conjunction event detection and collision risk assessment process by extending the covariance look-up-tables of the central tool CRASS. We analysed intrinsic TLE uncertainties for entire snapshots of a TLE catalogue. The applied method compares states derived directly from the TLE propagation with states resulting from an orbit determination using pseudo-observations derived from TLE data followed by a numerical propagation of the orbit determination result. The numerical propagation uses sophisticated force-models. The comparison is carried out in radial/along-track/out-of-plane components, revealing in some regions larger differences to the values used in CRASS. As expected, the TLE uncertainties are higher for elliptical orbits, in particular for low inclination values. The analysis also showed the existence of systematic patterns, most prominently observed as a inclination dependency of the along-track component in LEO.

This analysis is complemented by a validation of the obtained TLE orbit uncertainties for selected objects, for which precise orbits are available. We considered predictions from the ILRS, orbits determined from radar tracking of chaser objects involved in high-risk conjunction events, and orbits of objects regularly tracked by optical facilities at the Zimmerwald observatory. The validation of the estimated TLE uncertainties did not indicate the existence of systematic offsets for TLEs of objects in LEO, but showed that the results might be too optimistic

in some regions. For objects in the GEO region the TLE accuracy should be considered to be limited to some kilometers.

A comparison of the obtained TLE uncertainties from an analysis of historical TLE catalogue snapshots indicates a good consistency over the last 18 years. In the GEO region a degraded uncertainty over a few years has been observed, for which the reason is unknown. The further analysis of the TLE-accuracy in GEO might also subject to further studies, adressing also the consistency of subsequent TLE-sets.

We are now performing tests with CRASS using an accordingly updated and improved look-up table with the possibility of frequent object-wise updates, if needed. This future work will also help to address the applicability of the TLE theory to certain classes of orbits, in particular as function of individual sensor performance and observation scenarios, in order to select data product formats for the European Space Situational Awareness (SSA) system. We may already emphasise that the availability of reliable and up-to-date covariance information is essential for providing SSA-related products, such services forecasting conjunction events and estimating the collision risks.

REFERENCES

[1] J. R. Alarcón-Rodriguez, F. M. Martinez-Fadrique & H. Klinkrad (2004). Development of a collision risk assessment tool. Adv. Space Res., Vol. 34, No. 5, pp. 1120-1124.

[2] H. Klinkrad, J. R. Alarcón & N. Sanchez (2005). Collision Avoidance for Operational ESA Satellites. In Proc. 4th Europ. Conf. Space Debris (Ed. D. Danesy), ESA SP-587, pp. 509, ESA Publications Division, European Space Agency, Nordwijk, The Netherlands.

[3] T. Flohrer, H. Krag & H. Klinkrad (2009). ESA's Process for the Identification and Assessment of High-risk Conjunction Events. Paper submitted to Adv. Sp. Res.

[4] J. R. Alarcón-Rodriguez, H. Klinkrad, J. Cuesta & F. M. Martinez (2005). Independent Orbit Determination for Collision Avoidance. In Proc. 4th Europ. Conf. Space Debris (Ed. D. Danesy), ESA SP-587, pp. 331, ESA Publications Division, European Space Agency, Nordwijk, The Netherlands.

[5] H. Krag, H. Klinkrad & J. R. Alarcón-Rodriguez (2007). Assessment of Orbit Uncertainties for Collision Risk Predictions at ESA. Second IAASS conference "Space safety in a global world", 14 - 16 May 2007, Chicago, USA.

[6] T. Flohrer, H. Krag & H. Klinkrad (2008). Assessment and Categorization of TLE Orbit Errors for the US SSN Catalogue. In Proc. Advanced Maui Optical and Space Surveillance Technologies Conference, 17 - 19 September 2008, Wailea, Maui, USA.

[7] F. Laporte & E. Sasot (2008). Operational Management of Collision Risks for LEO satellites at CNES. AIAA 2008-3409, paper presented at the Space-Ops conference 12-16 May 2008, Heidelberg.

[8] R. Choc, H. Krag, H. Klinkrad & T. Flohrer (2009). Status of the ESA/ESOC Database and Information System Characterising Objects in Space (DISCOS) and its Web Front-end. In Proc. 5th Europ. Conf. Space Debris, ESA SP-672, ESA Publications Division, European Space Agency, Nordwijk, The Netherlands.

[9] T. Flohrer, H. Krag, H. Klinkrad, J. Kuusela, L. Leushacke, T. Schildknecht & M. Ploner (2009). Orbit Determination from Combined Radar and Optical Tracks during XMM Contingency Operation. In Proc. 5th Europ. Conf. Space Debris, ESA SP-672, ESA Publications Division, European Space Agency, Nordwijk, The Netherlands.

[10] M. R. Pearlman, J. J. Degnan & J. M. Bosworth (2002). The International Laser Ranging Service. Adv. Space Res., Vol. 30, No. 2, pp. 135-143.

[11] R. L. Ricklefs (2006). Consolidated Laser Ranging Prediction Format Version 1.01. available at http://ilrs.gsfc.nasa.gov/products_formats_procedures/predictions/cpf.html.

[12] P. Herridge, R. Khusul & J. Dick (2005). Confirming the Accuracy of Orbital Elements and Close-Approach Predictions in GEO. In Proc. 4th Europ. Conf. Space Debris (Ed. D. Danesy), ESA SP-587, pp. 337, ESA Publications Division, European Space Agency, Nordwijk, The Netherlands.